Increased Shear Stress Inhibits Angiogenesis in Veins and Not Arteries During Vascular Development.

Guillaume Chouinard-Pelletier[1], Espen D. Jahnsen[2], Elizabeth A.V. Jones[1,3]

[1]*Department of Chemical Engineering, McGill University, 3610 University St, Montreal, QC, Canada, H3A 2B2*

[2]*Department of Biomedical Engineering, McGill University, Duff Medical Building, 3755 University St, Rm316, Montreal, QC, Canada, H3A 2B4*

[3]*Lady Davis Institute, Jewish General Hospital, McGill University, 3755 Cote Ste- Catherine Rd, Montreal, QC, Canada, H3T 1E2*

Corresponding Author:

Elizabeth Jones

Lady Davis Institute

3755 Cote Ste-Catherine Rd.

Montreal, Qc, H3T 1E2, Canada

Tel: 514-398-4275

Fax: 514-398-6678

Email: liz.jones@mcgill.ca

Abstract

Vascular development is believed to occur first by vasculogenesis followed by angiogenesis. Though angiogenesis is the formation of new vessels, we found that vascular density actually decreases during this second stage. The onset of the decrease coincided with the entry of erythroblasts into circulation. We therefore measured the level of shear stress at various developmental stages and found that it was inversely proportional to vascular density. To investigate whether shear stress was inhibitory to angiogenesis, we altered shear stress levels either by preventing erythroblasts from entering circulation ("low" shear stress) or by injection of a starch solution to increase the blood plasma viscosity ("high" shear stress). By time-lapse microscopy, we show that reverse intussusception (merging of two vessels) is inversely proportional to the level of shear stress. We also found that angiogenesis (both sprouting and splitting) was inversely proportional to shear stress levels. These effects were specific to the arterial or venous plexus however, such that the effect on reverse intussusception was present only in the arterial plexus and the effect on sprouting only in the venous plexus. We cultured embryos under altered shear stress in the presence of either DAPT, a Notch inhibitor, or DMH1, an inhibitor of the BMP pathway. DAPT treatment phenocopied the inhibition of erythroblast circulation ("low" shear stress) and the effect of DAPT treatment could be partially rescued by injection of starch. Inhibition of the BMP signaling prevented the reduction in vascular density that was observed when starch was injected to increase shear stress levels.

***Keywords**: Vascular Development, Angiogenesis, Shear Stress, Vascular Remodeling, Particle Image Velocimetry*

List of Abbreviations

AF488	Alexa-Fluor 488
AcLDL	Acetylated Low Density Lipoprotein
Alk2/3	Activin receptor-like kinase 2/3
BMP	Bone morphogenetic protein
CAM	Chorio-Allantoic Membrane
DAPT	Notch Inhibitor N-[N-(3,5-Difluorophenacetyl)-L-alanyl]-S-phenylglycine t-butyl ester.
DMEM/F-12	Dulbecco's Modified Eagle Medium/ Nutrient Mixture F-12
DMH1	R-Smad Inhibitor 4-[6-(4-Isopropoxyphenyl)pyrazolo[1,5-a]pyrimidin-3-yl]quinoline, 4-[6-[4-(1-Methylethoxy)phenyl]pyrazolo[1,5-a]pyrimidin-3-yl]-quinoline
HEPES	4-(2-hydroxyethyl)-1-piperazineethanesulfonic acid
HUAEC	Human Umbilical Artery Endothelial Cell
HUVEC	Human Umbilical Vein Endothelial Cell
μPIV	Micro Particle Image Velocimetry
VEGF	Vascular Endothelial Growth Factor

Introduction

Angiogenesis is the process by which new blood vessels form and is essential to embryonic development. The first blood vessels of the embryo arise *de novo* through a process called vasculogenesis, which results in a network of blood vessels called the capillary plexus. These vessels are all approximately equal in diameter and morphologically distinct arteries and veins are absent. After the onset of blood flow, the vascular network remodels such that a hierarchical branching pattern becomes present and mural cells are recruited. The remodeling of the vasculature is dependent on blood flow and does not occur if blood flow is abnormal or stopped [1-3]. This second stage of vascular development is commonly referred to as angiogenesis. Though blood flow is required for this later stage of vascular development, surprisingly little is known about the effects of blood flow on angiogenesis. Our aim is to quantify angiogenesis during vascular remodeling and study the effect of blood flow on angiogenesis.

Controlling angiogenesis is an important therapeutic target for diseases such as macular degeneration and cancer. Angiogenesis is tightly regulated by both pro- and anti-angiogenic signals. Tissue growth creates regions of hypoxia, which is the strongest known stimulus for angiogenesis. Blood flow creates a force called shear stress that endothelial cells can sense and respond to. Shear stress has generally been considered to be pro-angiogenic since increases in blood flow induce the production of nitric oxide, a factor known to induce angiogenesis [4]. In exercise-induced angiogenesis models, the increased blood flow is thought to

be the primary stimulus for new vessel growth [5,6]. However, in a recent *in vitro* study by Song, *et al*, shear stress was shown to inhibit sprouting angiogenesis [7]. By subjecting a monolayer of endothelial cells seeded on a 3D collagen matrix to flow, they found a decrease in sprouting angiogenesis as compared to control. Although this work suggests that shear stress is a negative regulator of sprouting angiogenesis, an *in vitro* system cannot present the full complexity of a living organism and a more direct method of altering and visualizing angiogenesis and blood flow is required to study this interaction.

Changes in vessel density can occur through four different processes. New vessels form either by sprouting from an existing vessel or through the splitting of an existing vessel in two. Splitting angiogenesis (also called intussusception) is associated with altered blood flow patterns [8,9], and initiates with the formation of pillars in a blood vessel. Sprouting angiogenesis, on the other hand, is believed to be the prominent form induced by hypoxia [10]. Reductions in vascular density occur either by vascular regression or by reverse intussusception, which is the merging of two vessels into one. Discrepancies in the literature regarding the effect of shear stress on angiogenesis may be due to the exact forms of angiogenesis occurring in the different models. Exercise-induced angiogenesis is believed to occur by intussusceptive angiogenesis [5]. The *in vitro* system used by Song *et al*., on the other hand, did not allow for intussusceptive angiogenesis to occur and only looked at sprouting angiogenesis since the experimental model consisted of a mono-layer of cells rather than a capillary network [7].

Blood flow can have different effects on endothelial gene expression depending on the type of endothelial cell and flow present. Steady laminar flow induces

atheroprotective gene expression whereas oscillatory flow induces more atheroprone gene expression profiles [11]. Exposing endothelial cells derived from arteries and veins to the same flow results in different gene expression profiles as well [12]. Computational analysis of the flow patterns that are present during intussusceptive angiogenesis have predicted that pillars form in regions of flow recirculation [9]. Flow recirculation creates regions of low and oscillatory shear stress. For these reasons, it is likely that different types of flow patterns will have different effects on angiogenesis and that regional differences will also be present.

In this work, we have investigated the presence of angiogenesis during vascular remodeling in both avian and mammalian embryos. Surprisingly, we found that vascular density decreased during vascular remodeling and that this decrease began at the stage where erythroblasts entered circulation. We used time-lapse microscopy to quantitate angiogenesis (both vascular sprouting and intussusception) as well as vascular regression and the merging of two vessels (reverse intussusception). Interestingly, we found that even though the vascular density was reduced, significant angiogenesis was present (1.1 sprouts per mm^2 per hour). Since the reduction in vascular density correlated to the onset of erythroblast circulation, we measured shear stress during vascular remodeling and found that vascular density was inversely proportional to the magnitude of shear stress. We therefore altered shear stress to create situations of reduced or increased shear stress. We found that reverse intussusception (merging of two vessels) was inversely proportional to the shear stress condition but only in the arterial plexus. We observed increasing shear stress lead to a decrease in angiogenesis (both intussusceptive and sprouting) but only in the venous plexus.

Because of the differential effect between arteries and veins, we treated embryos undergoing vascular remodeling with a Notch inhibitor (DAPT). We found that Notch inhibition phenocopied the effect of reduced shear condition, and that injection of starch to increase shear in the presence of the Notch inhibitor partially rescued the phenotype. To investigate the effect of shear stress on veins, we inhibited the BMP pathways, which is known to be involved in the sprouting of veins but not arteries [13], using an R-Smad inhibitor (DMH1) and found that in the presence of the inhibitor, increased shear stress had no effect on vascular density whereas in the absence of the inhibitor a decrease is observed.

Methods

Branchpoint density

CD1 mice were mated overnight and the presence of a vaginal plug in the morning was taken as 0.5 days post coitus (dpc). Embryos were collected in a heated environment on the morning of the eighth or ninth day and dissected as described previously [14]. Briefly, dissecting medium was warmed to 37°C and placed in a tissue culture incubator for 15-30 minutes to allow the heart rate to recover.

Fertilized quail eggs (coturnix japonica) were incubated at 37°C and approximately 60% humidity for 40 to 72 hours as noted. A small amount of albumin was removed from the egg and a window was cut into the eggshell.

Both mouse and quail embryos were injected with Alexa-Fluor 488 (AF488)

conjugated dextran (Invitrogen). A picospritzer III (Parker) and small pulled glass microneedle with a tip diameter of approximately 10 μm was used to inject the solution (Sutter). The needle was inserted into vessels of the embryonic yolk sac and several pulses of solution were injected. The dye could be visualized during injection entering the heart and filling the vessels, ensuring delivery to only the cardiovascular system. Three to five yolk sacs per stage were analyzed. Images of the yolk sac vasculature were filtered and converted to binary images. Network morphology was quantified using Biologic Analyzer, a previously described software program developed by Nicolas Elie [15].

Time-Lapse Microscopy

After 40 hours of incubation (12-14 somites) chicken embryos were poured into a 60 mm Petri dish and injected with AF488-conjugated AcLDL (Invitrogen). A window large enough to expose the embryo was cut into the lid of the Petri dish. The window was covered with a thin Teflon membrane (YSI Incorporated) that was sealed to the lid with a layer of vacuum grease (Dow Corning). The Teflon membrane allows air to flow through, but is impermeable to liquid, thus preventing the embryo from drying out during imaging [16]. Embryos were moved to a temperature controlled upright fluorescence microscope and imaged once every 6 minutes for a maximum period of 10 hours using a 5x objective lens. A more detailed description of the protocol is published elsewhere (Al-Roubaie et al, Accepted, Dev Dyn).

Flow Dynamic Measurements

Previously published techniques for measuring mouse embryo hematocrit and

shear rate were used [17]. For quail embryos, 1 μm Fluospheres (Invitrogen) were injected into circulation using a picospritzer and a fine pulled needle as described above. Embryos were transferred to a fluorescent microscope equipped with an Ultima APX-RS camera and imaged for 1000 frames at 500 fps. These images were collapsed into one image and thresholded to a binary image in order to obtain an outline of the region with flow in the vessels. From the series of 1000 images, the period of systole was assessed visually and four frames were extracted from the observed peak velocities. Several individual vessel segments were cropped out of the larger images (Supplemental Figure 1A-B). Using uraPIV, an open source MatLab software developed by Roi Gurka, the speckle pattern in the vessel segments was analyzed for all image pairs. The interrogation window size and spacing was optimized for the vessel segment and based on a laminar flow profile the data from the best image pair was selected. It was necessary to analyze only vessel segments because PIV measurements are least accurate near walls and the majority of our measurements were located at the center of the vessels (Supplemental Figure 1C). We therefore assumed fully developed parabolic flow to calculate the shear rate. This assumption is valid based on the fact that embryonic blood flow is of very low Reynolds' number and Womersley number and therefore the entrance length of the blood vessel segment is on the order of microns [17,18]. The shear rate (γ) was calculated from:

$$\gamma = \frac{2V_{max}}{R}$$

The technique used to calculate hematocrit in avian embryos is similar to that used in mouse embryos [17]. Quail embryos were incubated to the appropriate stage, removed from the egg and placed in a 35 mm glass-bottom Petri dishes.

The embryos were injected with anionic 2,000,000MW fluorescein dextran (Invitrogen) using a fine pulled micro-needle and a picospritzer as described above. Embryos were then transferred to a heated confocal microscope stage. Hematocrit was measured by scanning the laser line over one single vessel rather than over the whole field of view. Against the fluorescent background of the plasma, the erythroblasts appear as dark streaks and the ratio of erythroblasts to plasma was used to estimate the hematocrit. We found that the hematocrit increased in a linear manner with somite stage (Supplemental Figure 1D). We used average hematocrit values for a given somite stage to estimate the blood viscosity. The viscosity of the flow was calculated using data from embryonic blood of chicken embryos at 4 days of development (Hamburger Hamilton stage 22), the youngest data available for embryonic blood viscosity [19].

Using the viscosity (μ) and the shear rate (γ) measurements, the shear stress (τ) was calculated from:

$$\tau = \mu\gamma$$

Immobilization of Blood Islands

Mouse embryos were day-mated and dissected in the morning of the 8th day of gestation (E8.0 or approximately 7-8 somites). Quail eggs were incubated for approximately 38 hours until the embryos reached 11-12 somites of development. The erythroblasts were sequestered in the blood islands using a method described in detail elsewhere [3]. Briefly, embryos were injected with a solution of 15% Acrylimide/bis-Acrylimide with 10 mM ammonium persulfate directly into the blood islands. A small amount of dye was added to the solution to visualize injection. In quail embryos, only the caudal blood islands were injected. Since the

blood islands surround the embryo in avians, polymerizing all the blood islands would have constrained growth of the embryo. The blood islands were then injected a second time with pure TEMED to catalyze the reaction. Embryos were either put in culture (for mice) or returned to the incubator (for quail) and dissected 16 hours later. Mouse embryos culture has been described in detail elsewhere [14]. The lack or reduction of erythroblast circulation was verified visually before dissection.

Hetastarch Injection

Mouse embryos were day-mated and dissected in the morning of the 8th day of gestation. Quail eggs were incubated for approximately 40 hours until the embryos reached 12-14 somites of development. Embryos were injected in the yolk sac with either Ringer's solution as a control or with 6% hetastarch (Sigma-Aldrich). A small amount of Texas-Red dextran (Invitrogen) was added to visualize injections (30% v/v). Mouse embryos were then placed in cultured for 16 hours as previously described [14]. Quail embryos were resealed and returned to the incubator for 14 hours.

Immunohistochemistry

The embryos were fixed with 4% PFA for quail embryos or Dent's fixative for mouse embryo. Mouse embryos were stained with biotinylated antibodies against CD31 (BD Bioscience) and quail embryos were stained with endothelial cell specific antibody QH1 (Iowa Developmental Hybridoma Banks). CD31 was detected with fluorescent streptavidin (Sigma) whereas AF488 anti-mouse secondary antibodies (Invitrogen) were used to detect QH1. Branchpoints were

evaluated as described above. Percent vascularized area was assessed by thresholding the images and measuring the number of white versus black pixels. For all embryos, 3-5 images per embryo were taken and averaged. Between 3 and 10 embryos, as noted, were included in each condition.

DAPT/DMH1 Treatment

Mouse embryos were day-mated and dissected in the afternoon of the 8th day of gestation. Embryos were injected either with saline control or hetastarch as described above. Embryos were placed in culture media with or without the presence of either 100 μM DAPT (Sigma) dissolved in DMSO or 10 μM DMH1 (Sigma) dissolved in DMSO. Embryos were dissected 16 hours later and stained for CD31 (BD Bioscience). Branchpoints and percent-vascularized area were evaluated as described above.

Results

To investigate the role of angiogenesis during vascular remodeling, we began by quantitating vascular density in the early embryo. The vasculature was highlighted by injection of fluorescently tagged dextran directly into the cardiovascular system in both mouse and quail embryos. The embryos were staged by counting the number of somites present. Somites are block-like structures that segment the embryo proper, and form regularly at a rate of one somite every 90 minutes such that they can be used to stage embryonic development. From images of the yolk sac vasculature, the total length of blood vessels, the density of branchpoints and the average vessel diameter was measured. In mouse embryos, we found that the

number of branchpoints, which is a measure of vascular density, increased before 8 somites after which a decrease in the number of branchpoints was observed (Figure 1A). The onset of circulation occurs in a step-wise manner; initially a period in which blood plasma flows but erythroblasts remain confined in the blood islands (3-5 somites in mouse), followed by a stage in which individual erythroblasts circulate intermittently (5-7 somites), and finally a stage at which continuous circulation is established (8 somites onward) [3,20]. Therefore, the decrease in branchpoints correlated to the onset of continuous erythroblast circulation. By 20 somites when morphologically distinct arteries and veins are present, the total vessel length and the total number of branchpoints began to increase again. A similar pattern was observed in the avian embryo where a decrease in the density of branchpoint was observed after the onset of blood flow (Figure 1B). In quail or chick, heart contraction begins at 8 somites [21] but erythroblasts do not enter circulation until approximately 11 somites. Due to technical limitations, we could not successfully inject dye before 12 somites and were unable to establish whether this decrease coincided with the entry of erythroblasts into circulation as occurs in the mouse embryo.

Since the vascular density decreased, we next investigated the presence of angiogenesis (both intussusceptive and sprouting) during vascular remodeling. The embryonic yolk sac is expanding during remodeling and therefore a lack of new vessel formation would result in a decrease in vascular density. Furthermore, vessels lacking flow are known to regress during embryonic development [22]. Intussusceptive growth of new blood vessels has also been documented during development [12] as well as reverse intussusception. Therefore, the reduction in vascular density could be the result of many different factors. As still images

cannot differentiate new vessel formation from vessel regression, time-lapse microscopy in chicken embryos was used to look at the morphological changes in the capillary plexus during vascular remodeling (Figure 2, Movie 1, n=6 embryos). We observed a significant number of new vessels forming by vascular sprouting (Figure 2C, Movie 1, red arrow). Filopodial extensions from endothelial cells are too small to be recognized at the magnification used (1.3 μm per pixel) and therefore these sprouts represent multi-cellular structures. We assessed the frequency of vessel regression, intussusception and reverse intussusception during remodelling (n=6 embryos). We found that vascular sprouting was in fact the most common event (1.09 sprouts per mm^2 per hour, ±0.16) as compared to vessel regression (0.19 vessel regressing per mm^2 per hour, ±0.06), intussusception (0.18 vessel splits per mm^2 per hour, ±0.03) and reverse intussusception (0.45 vessels merging per mm^2 per hour, ±0.07).

Since the decrease in vascular density correlated with the onset of erythroblast circulation, we measured wall shear stress levels in the first 24 hours of circulation. Shear stress is a factor of both shear rate, which is the velocity gradient of blood flow at the wall, and of the viscosity of the blood flow. For mouse embryos, we used a technique that we previously developed in which the laser of a confocal microscope is repeatedly scanned across one vessel and erythroblasts are marked using a mouse expressing GFP driven by the ε-globin promoter [17]. From these scans, both the hematocrit and the shear rate can be calculated to yield shear stress. All measurements were made in vessels of the capillary plexus. For quail embryos, micro-particle image velocimetry (μPIV) was used to analyze flow patterns in the embryonic capillary plexus. Embryos were injected with fluorescent micron-sized polystyrene beads and imaged using a

high-speed fluorescent microscope (500 fps, Supplemental Figure 1A). Measurements were done only on individual vessel segments and a parabolic velocity profile was assumed (see Methods). In both mouse and quail, we report average values at peak systole. We found that shear stress levels increased gradually after the onset of blood flow in both animal models. Shear stress levels peaked at 16-18 somites in mouse embryos (Figure 3A). In quail embryos, a maximum level was reached by 22-24 somites (Figure 3B). The levels of shear stress present in the blood vessels showed an inverse pattern to the density of branchpoints during vascular remodeling. We therefore plotted the shear stress at a given stage of development against the density of branchpoints at the same stage (Figure 3C-D). We found that a negative correlation was present between shear stress levels and the vascular density in both animal models.

Since shear stress is both a factor of the shear rate and the viscosity, we next altered shear stress levels in the embryo by altering the viscosity of the blood. The main viscous component of blood is the erythroblasts. Initially erythroblasts are confined to the blood islands. We previously developed a method to reduce the effective viscosity of circulating blood in mouse embryos by injection of a polymerizing agent into the blood islands to prevent their entry into circulation (see [3] and Methods). Only a partial sequestration of the erythroblasts is possible in avians (see Methods). We could increase shear stress by injection of a solution of hetastarch intra-vascularly in the presence of red blood cells to make the blood plasma more viscous. We have previously shown that injection of hetastarch solution into embryos can increase the viscosity of blood plasma [3]. Embryos were treated at 7-8 somites (mouse, n=10 control, n= 3 erythroblast immobilization and n=11 starch injection) or 12-14 somites (quail, n=6 control,

n= 4 erythroblast immobilization, n=6 starch injection), when erythroblasts normally enter circulation in each the respective animal models (see Methods). The embryos were allowed to develop for 16 hours and the number of branchpoints and the percent-vascularized area was evaluated. We found that sequestering the red blood cells in the blood islands resulted in a hyperfused vascular plexus (Figure 4A, red arrow) as compared to control resulting in an increase in the percent-vascularized area (Figure 4B). The same results were obtained in quail embryos (Figure 4C-D). We found that injection of hetastarch to make the blood plasma more viscous caused a significant decrease in branchpoints during the remodeling process without affecting the percent-vascularized area (Figure 4B, D).

Although our results show that vascular density was proportional to shear stress, the final vascular density is a consequence of many factors. Both a decrease in vascular sprouting or an increase in vessel regression would result in a decrease in final vascular density. Avian embryos were imaged by time-lapse microscopy under control, immobilization of the erythroblasts ("low" shear stress), or hetastarch injection ("high" shear stress) conditions in either the arterial or venous region of the capillary plexus (n=3 to 4 each in control/hetastarch/immobilization as well as arterial/venous for a total of 20 time-lapse movies). Under control conditions, vascular sprouting and intussusception occurred at the same rate in the arterial plexus as in the venous plexus (Figure 5). The arterial plexus presented a higher rate of vascular regression and reverse intussusception than the venous plexus. In the arterial plexus, immobilization of the erythroblasts resulted in a large increase in the presence of reverse intussusception (Movie 2) whereas hetastarch injection had the opposite effect resulting in a decrease in reverse

intussusception. Immobilization of erythroblasts also caused an increase in angiogenesis (both sprouting and intussusceptive) in the venous plexus with the opposite effect occurring after hetastarch injection. Neither treatment (immobilization or starch injection) had an effect on vascular sprouting in the arterial plexus. A large increase in vessel regression was observed in the venous plexus when we prevented erythroblast circulation but the opposite effect (i.e. decrease in regression) was not observed with hetastarch injection. As such, the level of reverse intussusception was inversely proportional to the level of shear stress present in the arterial plexus. The level of angiogenesis (both intussusceptive and sprouting) was inversely proportional to the level of shear stress in the venous plexus. The overall levels of intussusceptive angiogenesis were very low compared to sprouting angiogenesis.

Notch signalling is known to be involved in the differentiation of arteries. We therefore investigated the effect of inhibition of Notch signalling in the presence of altered shear stress levels using the γ-secretase inhibitor, DAPT (n=10 control, n=6 DAPT, n=7 hetastarch injection, n=6 DAPT & hetastarch injection). Mouse embryos treated with DAPT displayed a hyperfused yolk sac capillary plexus reminiscent of the results when erythroblasts were prevented from circulating (Figure 6A, red arrow). In fact, most of the plexus stained positive for CD31. In the most severe instances, regions of intense CD31 staining were present but no avascular regions (Supplemental Figure 2). The large increase in the percent vascularized area resulted in a decrease in the number of branchpoints present and an increase in the percent vascularized area (Figure 6E). When DAPT treatment was combined with intravascular injection of starch, a partial rescue of the phenotype was observed. Half of the yolk sac capillary plexus had normal

percent-vascularized area (Figure 6D, white arrow) whereas the rest of the plexus remained hyperfused.

After hetastarch injection, we observed a decrease in vascular density. The lower levels of reverse intussusception under this condition would actually lead to an increase in vascular density (i.e. if less vessels merge together than more branchpoints would be present). Therefore, the overall decrease observed must be the result of the decrease in angiogenesis present in the venous plexus after hetastarch injection. Bone morphogenetic protein (BMP) have been linked to sprouting from the venous plexus [13]. We inhibited the BMP pathway in mouse embryos using R-Smad inhibitor DMH1 in the presence of altered shear stress (Figure 7, n=10 control, n=6 DMH1, n=7 starch injection, n=5 DMH1 & starch injection). Unlike previously published results that showed that DMH1 treatment alone causes a decrease in vascular sprouting [13], we found no difference in vascular remodeling or vascular density after treatment with DMH1 (Figure 7B,E). When embryos were injected with starch and treated with DMH1, however, we failed to observe the decrease in vascular density observed when the starch is injected alone (Figure 7D, E).

Discussion

The traditional dogma of vascular development is that the vasculature forms by vasculogenesis followed by a stage of angiogenesis. Our results do show that a significant amount of angiogenesis is present during vascular remodeling. Our current time-lapse data is from an avian model, but we have also previously

published time-lapses of mammalian development (Movie 1 from [23]). In the mouse, vascular sprouting is present at a much lower level than we observed in the avian but it is present. The fact that the overall vascular density decreases, however, indicates that it is inappropriate to refer to this process as angiogenesis.

Shear stress is generally regarded as being pro-angiogenic; more specifically shear stress is thought to induce intussusceptive angiogenesis over sprouting angiogenesis. Using the chorio-allantoic membrane (CAM) of 16-day chicken embryos, Djonov *et al*. showed an increase in intussusceptive angiogenesis when flow through the CAM was increased by clamping one of the major side branches [8]. Though the ligation increased the overall flow, it also created regions where the altered flow patterns induced regions of recirculation and the authors have stated that they believe pillar formation was localized to regions of recirculation [24,9]. In the early embryo, there is a spatial separation between arteries and veins such that the caudal plexus is arterial and the rostral plexus is venous. The spatial separation allowed us to differentiate the effect of our starch injection experiments on the arterial and venous blood vessels independently. We found that intussusceptive angiogenesis in the arterial plexus is inversely proportional to the level of shear stress. We changed only the blood viscosity and not flow patterns, therefore it is difficult to compare our results to previously published findings. In agreement with the results of Song *et al*., we find that increased shear stress levels inhibit sprouting angiogenesis as well [7]. Interestingly, those experiments were performed with endothelial cells from a venous origin and our results suggest that a similar effect would not have been observed had endothelial cells from an arterial origin been used.

The overall phenotype of sequestering the erythrocytes to the blood islands was to cause an increase in vascularized area. From the time-lapse movies (Movie 2), we believe the observed phenotype is largely due to the increase in reverse intussusception in the arterial plexus. The effect of starch injection overall was to decrease vascular density. In this case, we believe the inhibition of angiogenesis in the veins dominates the phenotype since a decrease in reverse intussusception would result in a higher vascular density.

Though the pattern of blood flow changes between arteries and veins, it is also known that endothelial cells from arterial or venous origin react differently when the same type of flow is applied. *In vivo*, blood flow is pulsatile in arteries and is steady in veins. When endothelial cells of arterial origin (HUAECs; human umbilical artery endothelial cells) are exposed to pulsatile laminar flow *in vitro*, they increase the expression of genes involved in arterial identity, such as Hey1, ephrinB2, Dll1 and Nrp1 [12]. Application of steady flow to HUAECs has no effect on the expression of these same arterial genes. Conversely, neither steady nor pulsatile flow affect the expression of vein-specific gene CoupTF-II in HUAECS, but exposure of endothelial cells of venous origin (HUVECs; human umbilical vein endothelial cells) to steady flow induces an increase in CoupTF-II expression [12]. Our results are in agreement with these previously published results showing that arteries and veins react differently to the same hemodynamic stimuli.

Inhibition of Notch through the use of γ-secretase inhibitor DAPT phenocopied the effect of low shear stress and the effect of Notch inhibition could be partially rescued by the injection of starch to increase shear stress levels. We believe that

the DAPT treatment increased reverse intussusception in the yolk sac capillary plexus. The application of DAPT to avian embryos, which would have allowed us to time-lapse the phenotype easily, was not practical since the volume of the egg is large and the egg is viscous such that it would have been possible to mix the DAPT thoroughly. Our hypothesis is supported, however, by the presence of increased vascularized area, by the presence of punctate CD31 staining (Supplemental Figure 2), as well as by the fact that injection of hetastarch, which inhibits reverse intussusception, rescues the phenotype in the arterial plexus. We are not able to ascertain whether shear stress and Notch signaling activate the same pathway or parallel pathways in order to inhibit reverse intussusception. Though it is attractive to hypothesize that shear stress induces Notch that in turns inhibits reverse intussusception, the fact that shear stress can rescue the effect in the presence of the inhibitor contradicts this hypothesis. It is possible that Notch and shear stress can activate the same set of genes that are required for reverse intussusception. Alternatively, a more general mechanism, such as inhibiting endothelial cell replication, is responsible for the observed phenotype.

We found that the effects of altered shear stress on vascular sprouting were specific to the venous plexus. Sprouting from arteries has been linked to vascular endothelial growth factor (VEGF) expression whereas BMPs have been shown to be a vein-specific angiogenic cue [13]. In the presence of DMH1, injection of hetastarch did not induce a reduction in vascular density (Figure 7). Therefore our results indicate that shear stress can regulate sprouting in veins through the BMP pathway. The one caveat regarding this interpretation of the results is that no effect was observed with DMH1 alone. Shear stress is present even without hetastarch injection. Based on the results during normal development (Figure 1,

3), we would expect increased vascular density with DMH1 alone as compared to control. We did observe a very small increase, but it was not statistically significant. It is also possible that the dose used only partially inhibited the BMP pathway. DMH1 inhibits Smad phosphorylation by inhibiting the kinase activity of Activin receptor-like kinase 2/3 (Alk2/3) [25]. The fact that DMH1 inhibits shear-induced change in vascular density raises the interesting possibility that Alk2/3 can be activated in a ligand-independent manner in veins, similar to the activation of VEGFR2 in a ligand-independent manner by shear stress [26]. We currently cannot exclude the possibility, however, that altered shear stress changes the expression of BMP proteins rather than affecting the receptor directly. BMPs have also been implicated in the balance between maturation of blood vessels and new vessel formation by differential expression of BMP family members [27]. Since shear stress is an important signal for vessel maturation, it is reasonable to hypothesize that shear stress would be responsible for the differential expression of these BMPs during vascular remodeling.

Our measurements of shear stress in the mouse embryonic plexus are similar to previously reported levels in embryos [17,28]. Our results in the quail embryo are slightly higher than previously reported values for avian embryos [28]. We used μPIV to measure flow in small segments of the vasculature, assuming a parabolic flow profile. This assumption is most likely valid and several groups have shown that parabolic velocity profiles exist throughout the cardiac cycle in embryonic blood vessels [17,29]. We also assumed average hematocrit values for each somite stage for the avian data. Vessels with diameters less than 300 μm are known to have lower effective viscosities due to the Fahreus-Lindqvist effect [30]. Though assuming a constant viscosity for all vessels is common in the literature

[31,28], this assumption could lead to slight overestimates of the shear stress values. Therefore, it is possible that our shear stress measurements in quail are a slight overestimation. In the mouse, we observed a decrease in the shear stress levels after 16 somites. In the avian, the level of shear stress is slightly lower at 24 somites than at 22 somites though this difference is not statistically significant. Remodeling creates a more hemodynamically efficient network with less resistance to flow and therefore lower levels of shear stress will be present. If shear stress levels decrease after 22 somites (as observed in the mouse embryo after 16 somites), our shear stress measurement may be higher because we are measuring shear stress levels in younger embryos than previously reported (30-35 somites) and not because of errors in our PIV measurements [32-34,28].

In our experimental system, we used immobilization of erythroblasts in the blood islands to make the blood less viscous and the injection of a starch solution to make the blood plasma more viscous. Erythroblasts also carry oxygen and we cannot rule out a role for oxygen in this system. In our previous work, we prevented erythroblasts from entering circulation during development and showed that the entry of erythroblasts was essential for vascular remodeling to occur [3]. We then injected embryos in which we had prevented erythroblast circulation with hetastarch to normalize the viscosity of the blood in the absence of red blood cells. In these embryos, vascular remodeling was rescued. Based on those results, we believe the effect is largely due to altered hemodynamic signalling. Hetastarch, on the other hand, also affects plasma osmolality and we cannot rule out that changes in osmolality are playing a role in the observed phenotype. The experimental system is limited by the fact that we cannot measure the viscosity of the blood. The embryos are too small to collect more than ~1 μL of blood.

Considering that in wild-type embryos vascular density is proportional to shear stress and considering that the immobilization of erythroblasts has the opposite effect to the injection of hetastarch, our evidence strongly supports that the observed effects are due to altered hemodynamic force.

Conclusions

Our results show that vascular remodeling is accompanied by a reduction in vascular density and that this reduction begins when erythroblasts enter circulation. This is contrary to the idea that vascular remodeling occurs by a process of angiogenesis. We do find that angiogenesis is present during vascular remodeling however referring to remodeling as "angiogenesis" is an over-simplification. We report the first measurements of changes in shear stress during vascular remodeling. We find the shear stress levels correlate to the vascular density and that increased shear stress during vascular remodeling results in a decrease in vascular density. We find that reverse intussusception (or the merging of two vessels) is inhibited by increasing levels of shear stress in the atrial plexus. Inhibition of Notch signaling also results in a hyperfused plexus but the effects of Notch inhibition can be partially rescued by increasing shear stress levels. In the venous plexus, we find that increasing levels of shear stress inhibit vascular sprouting through a BMP-dependent pathway.

Acknowledgements

This work was supported by grants from the Natural Science and Engineering Research Council's Discovery Program (342134), the Fonds de recherche du Québec - Nature et technologies'

Nouveau Chercheur Program (131373) and the Canadian Foundation for Innovation. The Eugenie Lamothe Fellowship supported GCP and EDJ.

References

1. Chapman WB (1918) The effect of the heart-beat upon the development of the vascular system in the chick. Am J Anat 23:175-203
2. Huang C, Sheikh F, Hollander M, Cai C, Becker D, Chu PH, Evans S, Chen J (2003) Embryonic atrial function is essential for mouse embryogenesis, cardiac morphogenesis and angiogenesis. Development 130 (24):6111-6119
3. Lucitti JL, Jones EA, Huang C, Chen J, Fraser SE, Dickinson ME (2007) Vascular remodeling of the mouse yolk sac requires hemodynamic force. Development 134 (18):3317-3326
4. Ziche M, Morbidelli L, Choudhuri R, Zhang HT, Donnini S, Granger HJ, Bicknell R (1997) Nitric oxide synthase lies downstream from vascular endothelial growth factor-induced but not basic fibroblast growth factor-induced angiogenesis. J Clin Invest 99 (11):2625-2634. doi:10.1172/JCI119451
5. Brown MD, Hudlicka O (2003) Modulation of physiological angiogenesis in skeletal muscle by mechanical forces: involvement of VEGF and metalloproteinases. Angiogenesis 6 (1):1-14
6. Carrow RE, Brown RE, Van Huss WD (1967) Fiber sizes and capillary to fiber ratios in skeletal muscle of exercised rats. Anat Rec 159 (1):33-39. doi:10.1002/ar.1091590106
7. Song JW, Munn LL (2011) Fluid forces control endothelial sprouting. Proc Natl Acad Sci U S A 108 (37):15342-15347. doi:10.1073/pnas.1105316108
8. Djonov V, Schmid M, Tschanz SA, Burri PH (2000) Intussusceptive angiogenesis: its role in embryonic vascular network formation. Circ Res 86 (3):286-292.
9. Lee GS, Filipovic N, Miele LF, Lin M, Simpson DC, Giney B, Konerding MA, Tsuda A, Mentzer SJ (2010) Blood flow shapes intravascular pillar geometry in the chick chorioallantoic membrane. J Angio Res 2:11. doi:10.1186/2040-2384-2-11
10. Styp-Rekowska B, Hlushchuk R, Pries AR, Djonov V (2011) Intussusceptive angiogenesis: pillars against the blood flow. Acta Physiol (Oxf) 202 (3):213-223. doi:10.1111/j.1748-1716.2011.02321.x
11. Resnick N, Yahav H, Shay-Salit A, Shushy M, Schubert S, Zilberman LCM, Wofovitz E (2002) Fluid shear stress and the vascular endothelium: for better and for worse. Prog Biophys Mol Biol 81 (3):177-199
12. Buschmann I, Pries A, Styp-Rekowska B, Hillmeister P, Loufrani L, Henrion D, Shi Y, Duelsner A, Hoefer I, Gatzke N, Wang HT, Lehmann K, Ulm L, Ritter Z, Hauff P, Hlushchuk R, Djonov V, van Veen T, Le Noble F (2010) Pulsatile shear and Gja5 modulate arterial identity and remodeling events during flow-driven arteriogenesis. Development 137 (13):2187-2196. doi:Doi 10.1242/Dev.045351
13. Wiley DM, Kim JD, Hao J, Hong CC, Bautch VL, Jin SW (2011) Distinct signalling pathways regulate sprouting angiogenesis from the dorsal aorta and the axial vein. Nat Cell Biol 13 (6):686-692. doi:10.1038/ncb2232
14. Jones EA, Crotty D, Kulesa PM, Waters CW, Baron MH, Fraser SE, Dickinson ME (2002) Dynamic in vivo imaging of postimplantation mammalian embryos using whole embryo culture. Genesis 34 (4):228-235.
15. Jones EA, Yuan L, Breant C, Watts RJ, Eichmann A (2008) Separating genetic and hemodynamic defects in neuropilin 1 knockout embryos. Development 135 (14):2479-2488
16. Kulesa PM, Fraser SE (2000) In ovo time-lapse analysis of chick hindbrain neural crest cell migration shows cell interactions during migration to the branchial arches. Development 127 (6):1161-1172.
17. Jones EA, Baron MH, Fraser SE, Dickinson ME (2004) Measuring hemodynamic changes during mammalian development. Am J Physiol Heart Circ Physiol 287 (4):H1561-1569
18. Phoon CK, Aristizabal O, Turnbull DH (2002) Spatial velocity profile in mouse embryonic aorta and Doppler-derived volumetric flow: a preliminary model. Am J Physiol Heart Circ Physiol 283 (3):H908-916.
19. Al-Roubaie S, Jahnsen ED, Mohammed M, Henderson-Toth C, Jones EA (2011) Rheology of embryonic avian blood. Am J Physiol Heart Circ Physiol 301 (6):H2473-2481. doi:10.1152/ajpheart.00475.2011

20. McGrath KE, Koniski AD, Malik J, Palis J (2003) Circulation is established in a stepwise pattern in the mammalian embryo. Blood 101 (5):1669-1676
21. Hirota A, Fujii S, Kamino K (1979) Optical monitoring of spontaneous electrical activity of 8-somite embryonic chick heart. Jap J Physiol 29 (5):635-639
22. Clark ER (1918) Studies on the growth of blood-vessels in the tail of the frog larva - By observation and experiment on the living animal. Am J Anat 23 (1):37-88
23. Jones EA, le Noble F, Eichmann A (2006) What determines blood vessel structure? Genetic prespecification vs. hemodynamics. Physiology 21:388-395
24. Djonov VG, Kurz H, Burri PH (2002) Optimality in the developing vascular system: branching remodeling by means of intussusception as an efficient adaptation mechanism. Dev Dyn 224 (4):391-402
25. Hao J, Ho JN, Lewis JA, Karim KA, Daniels RN, Gentry PR, Hopkins CR, Lindsley CW, Hong CC (2010) In vivo structure-activity relationship study of dorsomorphin analogues identifies selective VEGF and BMP inhibitors. ACS Chem Biol 5 (2):245-253. doi:10.1021/cb9002865
26. Jin ZG, Ueba H, Tanimoto T, Lungu AO, Frame MD, Berk BC (2003) Ligand-independent activation of vascular endothelial growth factor receptor 2 by fluid shear stress regulates activation of endothelial nitric oxide synthase. Circ Res 93 (4):354-363. doi:10.1161/01.RES.0000089257.94002.96
01.RES.0000089257.94002.96 [pii]
27. David L, Feige JJ, Bailly S (2009) Emerging role of bone morphogenetic proteins in angiogenesis. Cytokine Growth Factor Rev 20 (3):203-212. doi:10.1016/j.cytogfr.2009.05.001
28. Poelma C, Vennemann P, Lindken R, Westerweel J (2008) In vivo blood flow and wall shear stress measurements in the vitelline network. Exp Fluid 45 (4):703-713. doi:DOI 10.1007/s00348-008-0476-6
29. Larina IV, Sudheendran N, Ghosn M, Jiang J, Cable A, Larin KV, Dickinson ME (2008) Live imaging of blood flow in mammalian embryos using Doppler swept-source optical coherence tomography. J Biomed Opt 13 (6):060506. doi:10.1117/1.3046716
30. Fahraeus R, Lindqvist T (1931) The viscosity of blood in narrow capillary tubes. Am J Physiol 99:563-568
31. Poelma C, Van der Heiden K, Hierck BP, Poelmann RE, Westerweel J (2010) Measurements of the wall shear stress distribution in the outflow tract of an embryonic chicken heart. J R Soc Interface 7 (42):91-103. doi:rsif.2009.0063 [pii]
10.1098/rsif.2009.0063
32. Davis A, Izatt J, Rothenberg F (2009) Quantitative measurement of blood flow dynamics in embryonic vasculature using spectral Doppler velocimetry. Anat Rec (Hoboken) 292 (3):311-319. doi:10.1002/ar.20808
33. Lee JY, Ji HS, Lee SJ (2007) Micro-PIV measurements of blood flow in extraembryonic blood vessels of chicken embryos. Physiol Meas 28 (10):1149-1162. doi:S0967-3334(07)46812-5 [pii]
10.1088/0967-3334/28/10/002
34. Lee JY, Lee SJ (2010) Hemodynamics of the omphalo-mesenteric arteries in stage 18 chicken embryos and "flow-structure" relations for the microcirculation. Microvasc Res 80 (3):402-411. doi:10.1016/j.mvr.2010.08.003

Figure Legends

Figure 1 - Vascular Density Decreases During Vascular Remodeling in Both Mammalian and Avian Embryos. The morphology of the yolk sac vasculature was visualized by injection of fluorescent dextrans at different stages of development. The density of branchpoints per unit area was calculated and plotted with respect to somite stage between 5 somites and 25 somites in mouse embryos (A) and between 12 and 24 somites in quail embryos (B). The branchpoint density increased until 8 somites in the mouse and then decreased between 8 and 22 somites. The initiation of the decrease in vascular density correlated with the onset of continuous erythroblast circulation [3]. A similar pattern was observed in the quail embryos where vascular density decreased after the onset of erythroblast circulation.

Figure 2 – Time-lapse Microscopy of Vascular Remodeling in Avian Embryos Demonstrate that Significant Angiogenic Sprouting is Present. The extra-embryonic vasculature of a chicken embryo was labeled by injection of AF488-acLDL at 12 somites, just before the onset of erythroblast circulation (A). The embryo was kept alive on a heated microscope using a modification to a previously published technique [16]. During remodeling, the formation of the major artery of the yolk sac can be observed (B) as well as significant amounts of angiogenesis (C, arrows). The lower panels (C) show the region highlighted by the blue box (A,B) and various time points. The panels exemplify the sprouting angiogenesis that is observed during embryonic vascular development. Scale bar: 200 μm (A,B), 100 μm (C).

Figure 3 – Vascular Density is Inversely Proportional to Shear Stress During Development. Combining velocity measurements and hematocrit measurements, the amount of shear stress was calculated for vessels of the embryonic yolk sac with respect to somite stage for both mouse (A) and quail embryos (B). In mouse, shear stress levels increased after the onset of blood flow, reaching a peak at 16 somites. In quail embryos, the level of shear stress increased until 22 somites. The total number of branchpoints was then plotted with respect to the level of shear stress present at a given stage of development for both mouse (C) and quail embryos (D). A negative correlation was found between the number of vessels and the amount of shear stress present.

Figure 4 – Increasing Plasma Viscosity During Vascular Remodeling in Avian Embryos Leads to a Decrease in Vascular Density. Mouse embryos (A,B) and quail embryos (C,D) were injected with either Ringer's Solution (control), subjected to erythroblasts immobilization in the blood islands to reduce shear stress levels (RBC Immobilization) or injected with 6% hetastarch to

increase plasma viscosity and therefore shear stress levels (Hetastarch Injected) and allowed to develop for 16 hours. Embryos were fixed and stained with either for CD31 (mouse, A) or an endothelial specific antibody called QH1 (quail, C) to highlight the vasculature. The number of branchpoints per unit area and the percent-vascularized area was measured for each group (B, D). The injection of the starch caused a significant decrease in the density of branchpoints in both animal models. The immobilization of erythroblasts resulted in a hyperfused vascular plexus (A, red arrow) such that the percent-vascularized area was significantly increased. Scale bar: 500 μm (A), 200 μm (C). * $p<0.05$, ** $p<0.01$, *** $p<0.001$.

Figure 5 – Lowering Shear Stress Increases Reverse Intussusception in Arterial Plexus Whereas Increasing Shear Stress Inhibits Vascular Sprouting in the Venous Plexus. The presence of sprouting, intussusception, regression and reverse intussusception was assessed by time-lapse microscopy both during normal development and under altered hemodynamic conditions. Shear stress was reduced by preventing the entry of erythroblasts into circulation and increased by injection of hetastarch solution to make the blood plasma more viscous. Only a partial sequestration of the erythroblasts is possible in avians (see Methods). During early vascular development, the arterial and venous plexus are spatially separated with arteries at the caudal end of the embryo and venous vessels at the rostral end. Time-lapse images were therefore identified as either arterial or venous. We find reverse intussusception is increased after erythroblast immobilization and decreased after hetastarch injection in the arterial plexus but not the venous plexus. We find increased vascular sprouting in the venous plexus when erythroblasts are immobilized and a decrease in vascular sprouting when hetastarch is injected but no decrease is observed in the arterial plexus.

Figure 6 – Inhibition of Notch Signaling Phenocopies The Effect of Low Shear Stress And Can Be Partially Rescued by Injection of Hetastarch. Mouse embryos were cultured with or without the presence of DAPT, a selective γ-secretase inhibitor that blocks the Notch signaling pathways. Shear stress was also altered by the injection of hetastarch to increase plasma viscosity. Embryos were then cultured for 16 hours and stained with antibodies against CD31 (A-D). Control embryos display a remodeled vascular network (A), whereas DAPT treatment results in a hyperfused vascular network (B, red arrow) with an increase in the percentage of CD31+ area within the vascular network (E). Injection of Hetastarch (C) resulted in a small but statistically significant decrease in vascular density (E). The combination of hetastarch injection with DAPT treatment resulted in a partial rescue of vascular development (D) such that hyperfused plexus was not present in half the yolk sac (white arrow). Both the values for branchpoints density and the percent-vascularized area were closer to control when both starch injection and DAPT treatment were administered as compared to DAPT alone (E). Scale bar: 1000 μm * $p<0.05$, ** $p<0.01$, *** $p<0.001$.

Figure 7 – Inhibiting BMP Signaling Pathway Prevents Shear Stress Induced Reduction in Vascular Density. Mouse embryos were cultured with or without the presence of DMH1, an inhibitor of Alk2/3 kinase activity. Shear stress was also altered by the injection of hetastarch to increase plasma viscosity. Embryos were cultured for 16 hours and stained with antibodies against CD31 (A-D) and the density of branchpoints and percent vascularized area was measured (E). Control embryos display a remodeled vascular network with normal vascular density in arteries and veins (A). DMH1 treatment alone did not appear to affect vascular development (B, E). Injection of starch solution to increase plasma viscosity resulted in a decrease in vascular density in veins (C, E). When starch solution was injected in the presence of DMH1, no decrease in vascular density was observed (D, E). Scale bar: 100 μm. ** $p<0.01$

Movie Legend

Movie 1 – Time-lapse of Vascular Remodeling in Avian Embryos. Chicken embryos were followed by *ex ovo* time-lapse microscopy. Eggs were incubated until the embryo reached 12-14 somites. Embryos were then injected with AF488-AcLDL, which labels endothelial cells and macrophages. The embryos were transferred to a petri dish in which a Teflon covered window was made into the lid (see Methods). Embryos were transferred to a heated fluorescent microscope and an image was taken every 6 minutes for 10 hours using a 5x objective lens. The movies are played at 8 frames per second. The arrows highlight the presence of sprouting angiogenesis (red arrow) and reverse intussusception (yellow arrow). Scale bar: 200 μm.

Movie 2 – Time-lapse of Vascular Remodeling Under Low Shear Stress in Avian Embryos. Eggs were incubated until the embryo reached 12-14 somites and then injected with AF488-AcLDL, which labels endothelial cells and macrophages. The erythroblasts at the caudal end of the yolk sac were prevented from entering circulation by injection of Acrylimide/APS followed by injection of TEMED (See Methods). This reduced the effective hematocrit of the blood flow. The embryos were then transferred to a petri dish in which a Teflon covered window was made into the lid (see Methods). An image was taken every 10 minutes for 10 hours using a 10x objective lens. The movies are played at 8 frames per second. Under low shear stress, significant amounts of reverse intussusception are present (white, yellow and red arrows). Scale bar: 100 μm.

Figure 1

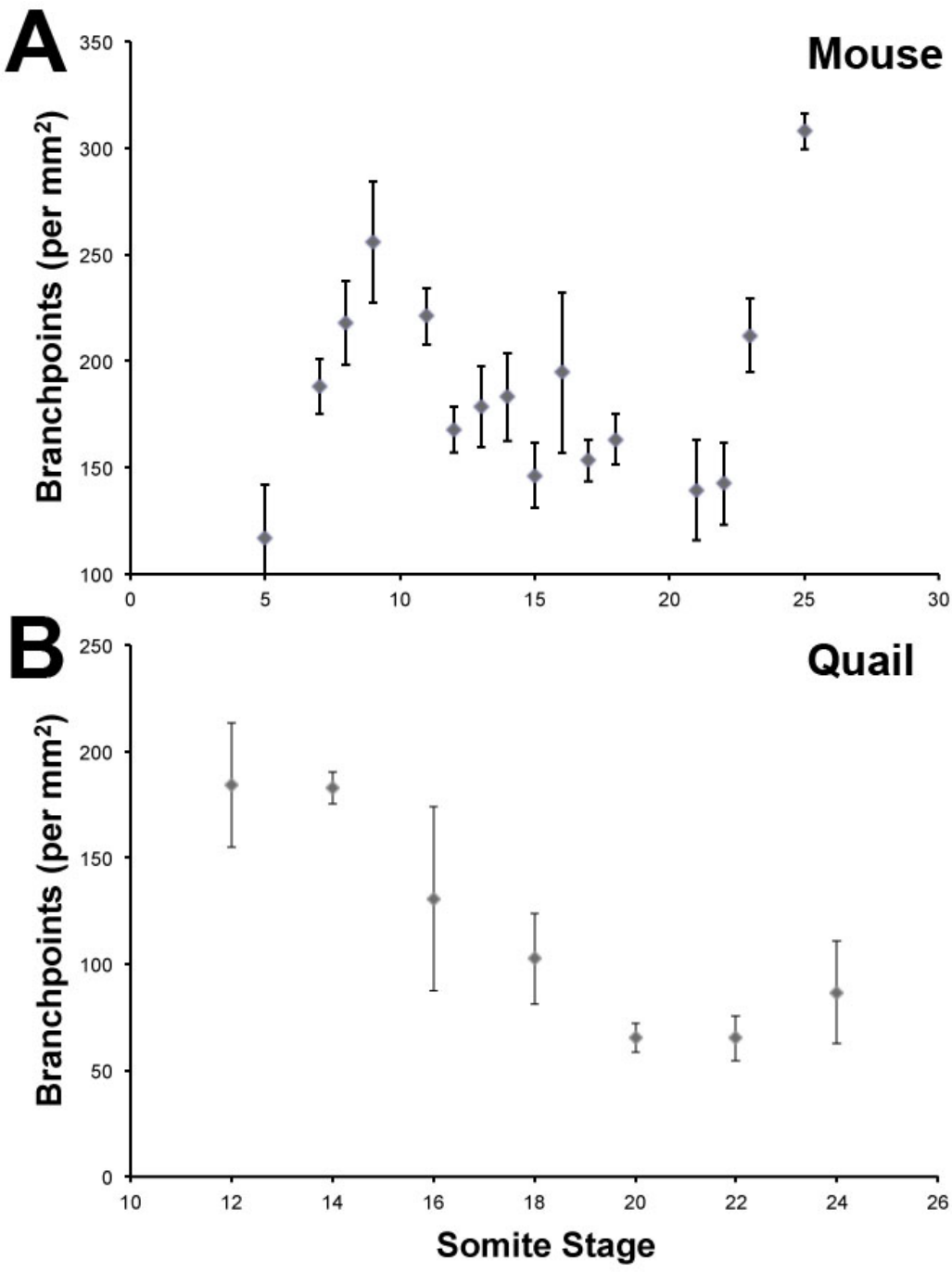
A
Mouse
Branchpoints (per mm²)
350
300
250
200
150
100
0
5
10
15
20
25
30
B
Quail
Branchpoints (per mm²)
250
200
150
100
50
0
10
12
14
16
18
20
22
24
26
Somite Stage

Figure 2

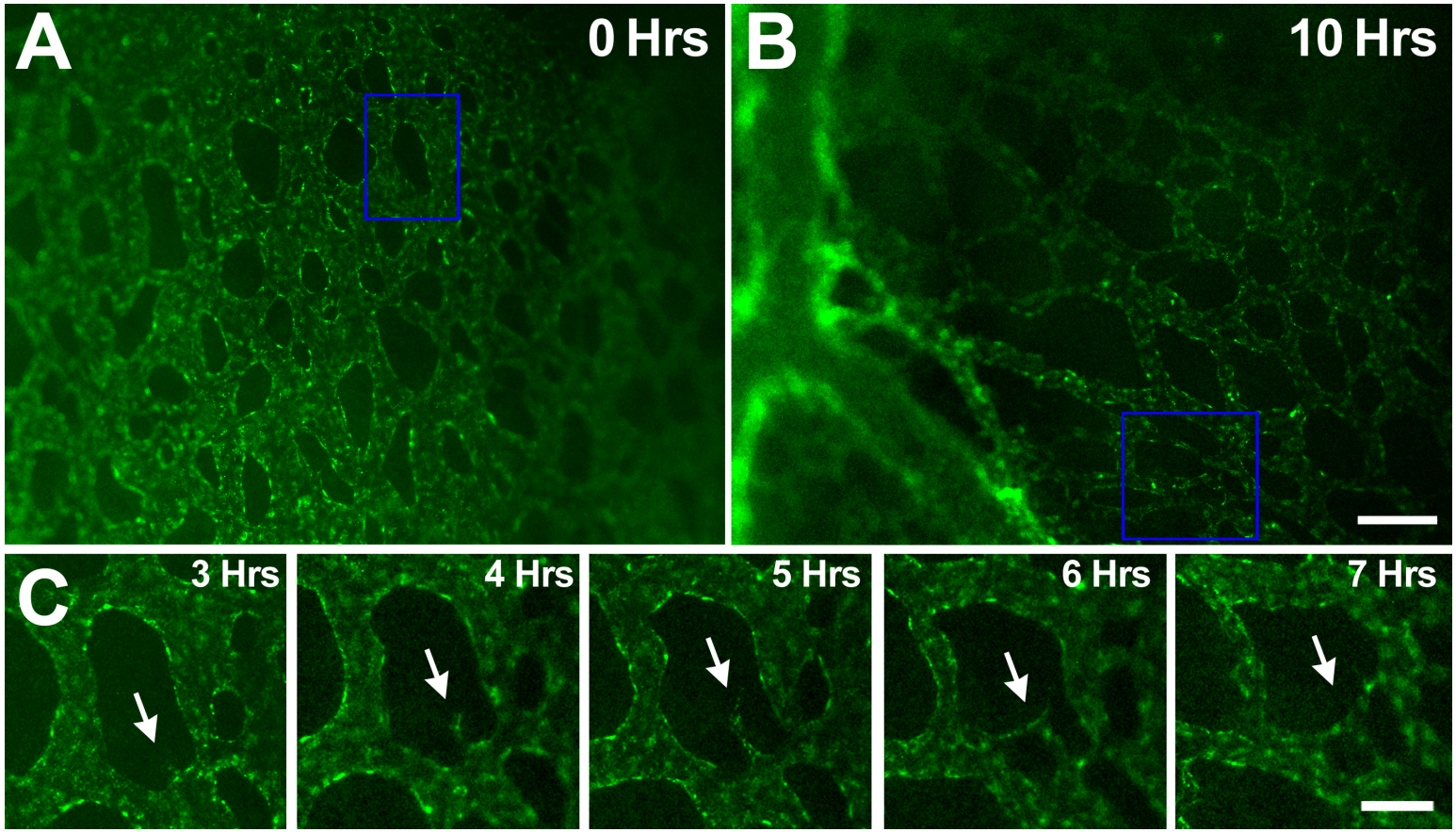

Figure 3

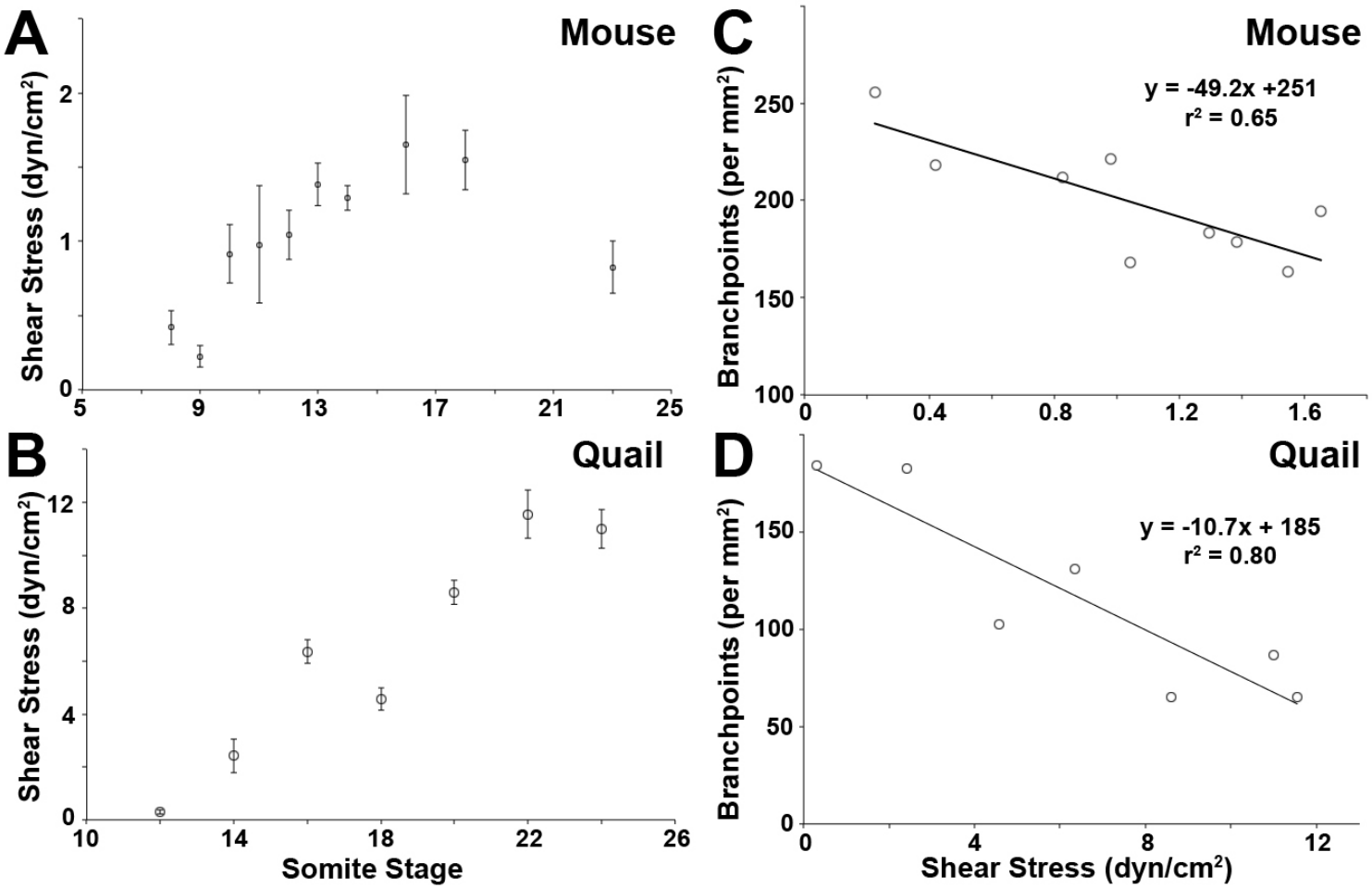
A
Mouse
Shear Stress (dyn/cm²)
0
1
2
5
9
13
17
21
25
B
Quail
Shear Stress (dyn/cm²)
0
4
8
12
10
14
18
22
26
Somite Stage
C
Mouse
y = -49.2x +251
r² = 0.65
Branchpoints (per mm²)
100
150
200
250
0
0.4
0.8
1.2
1.6
D
Quail
y = -10.7x + 185
r² = 0.80
Branchpoints (per mm²)
0
50
100
150
0
4
8
12
Shear Stress (dyn/cm²)

Figure 4

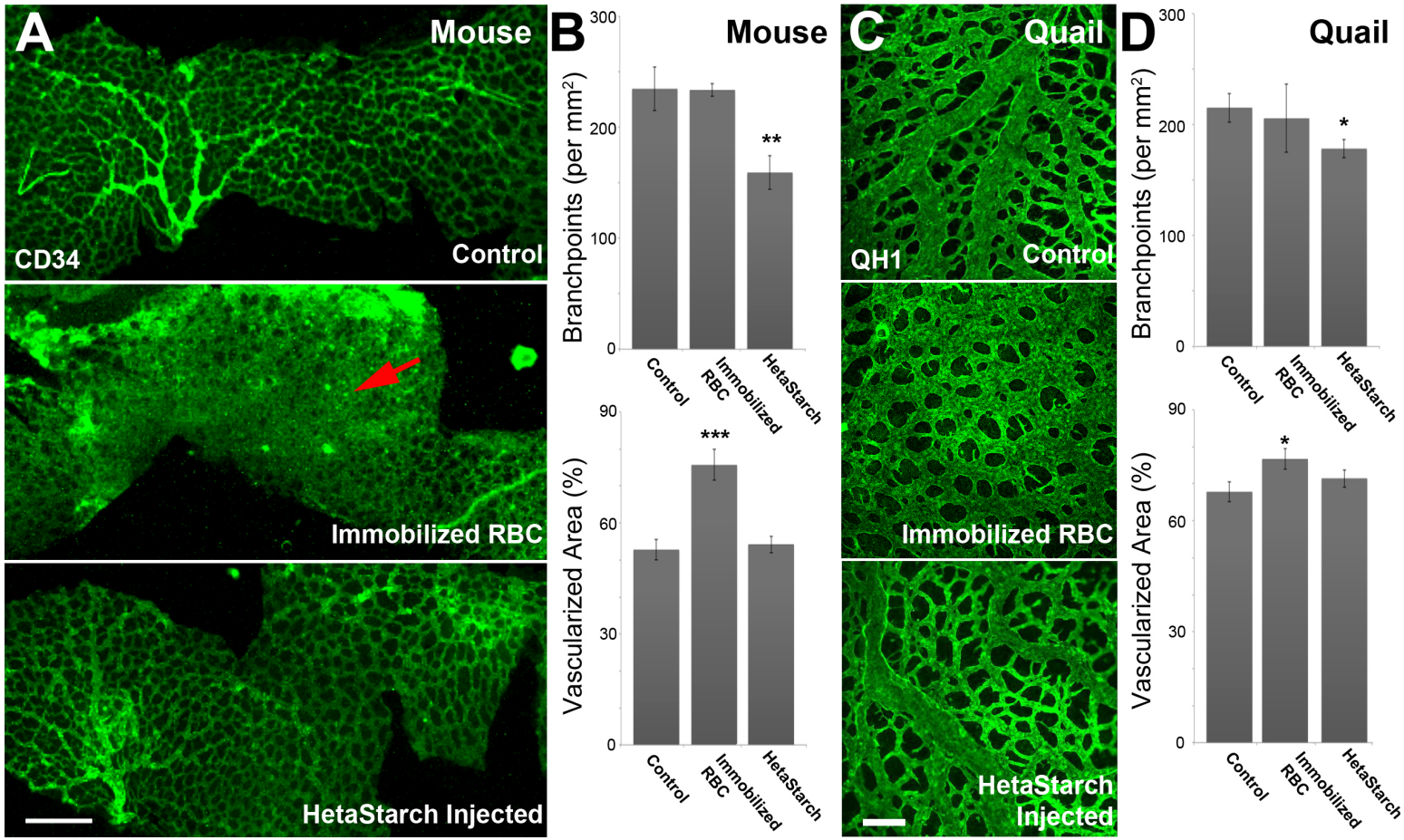
A
Mouse
CD34
Control
Immobilized RBC
HetaStarch Injected
B
Mouse
Branchpoints (per mm²)
300
200
100
0
**
Control
Immobilized RBC
HetaStarch
Vascularized Area (%)
90
60
30
0
***
Control
Immobilized RBC
HetaStarch
C
Quail
QH1
Control
Immobilized RBC
HetaStarch Injected
D
Quail
Branchpoints (per mm²)
300
200
100
0
*
Control
Immobilized RBC
HetaStarch
Vascularized Area (%)
90
60
30
0
*
Control
Immobilized RBC
HetaStarch

Figure 5

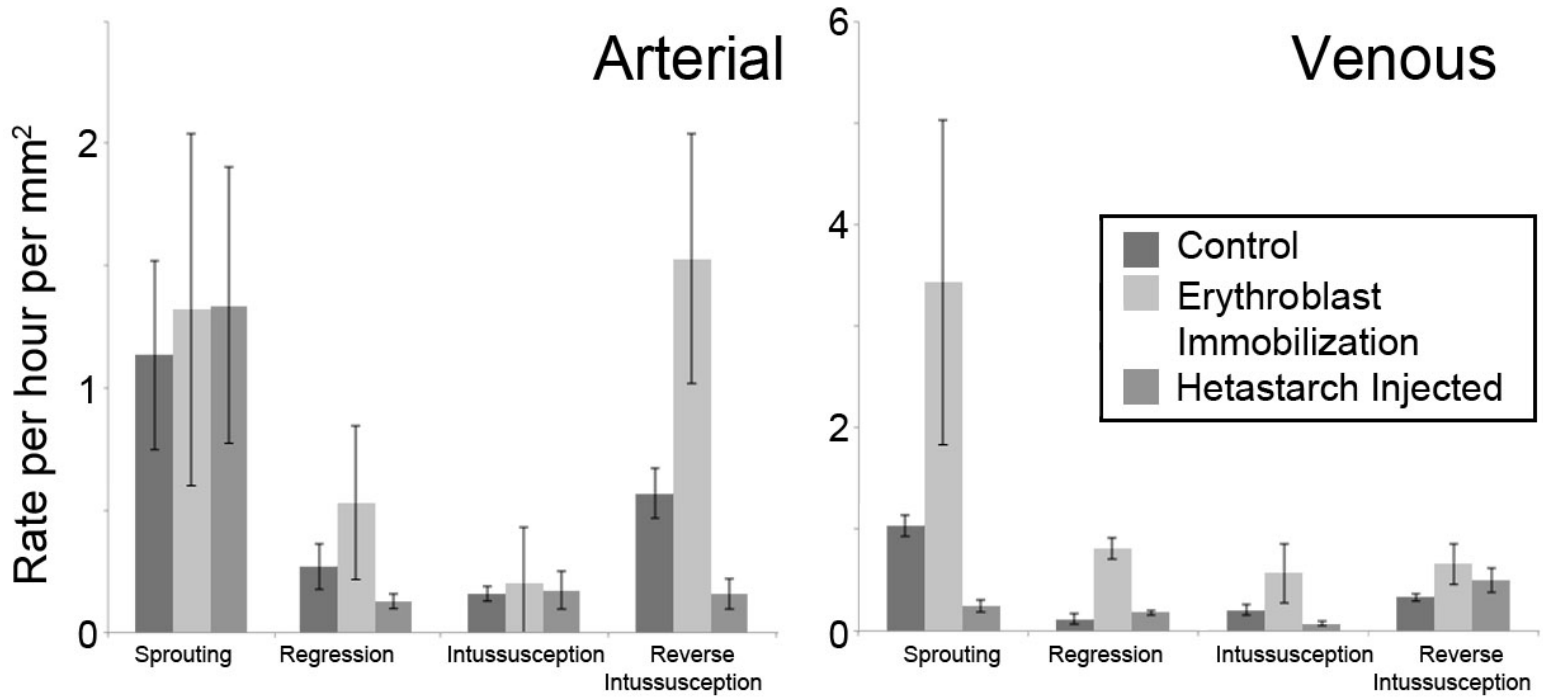
Arterial
Venous
Rate per hour per mm²
0
1
2
0
2
4
6
Control
Erythroblast
Immobilization
Hetastarch Injected
Sprouting
Regression
Intussusception
Reverse
Intussusception
Sprouting
Regression
Intussusception
Reverse
Intussusception

Figure 6

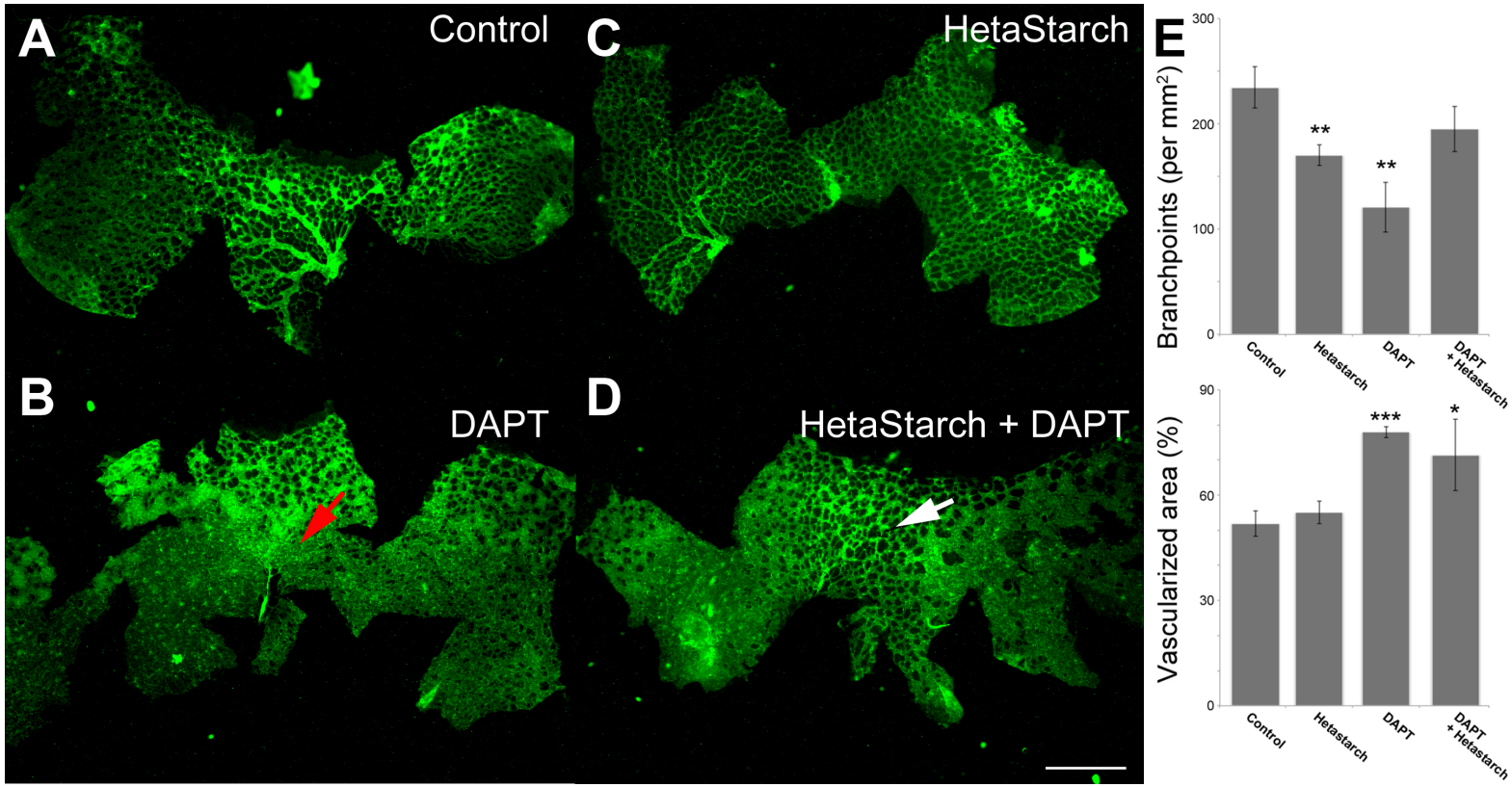
A
Control
C
HetaStarch
B
DAPT
D
HetaStarch + DAPT
E
Branchpoints (per mm²)
300
200
100
0
**
**
Control
Hetastarch
DAPT
DAPT + Hetastarch
Vascularized area (%)
90
60
30
0
***
*
Control
Hetastarch
DAPT
DAPT + Hetastarch

Figure 7

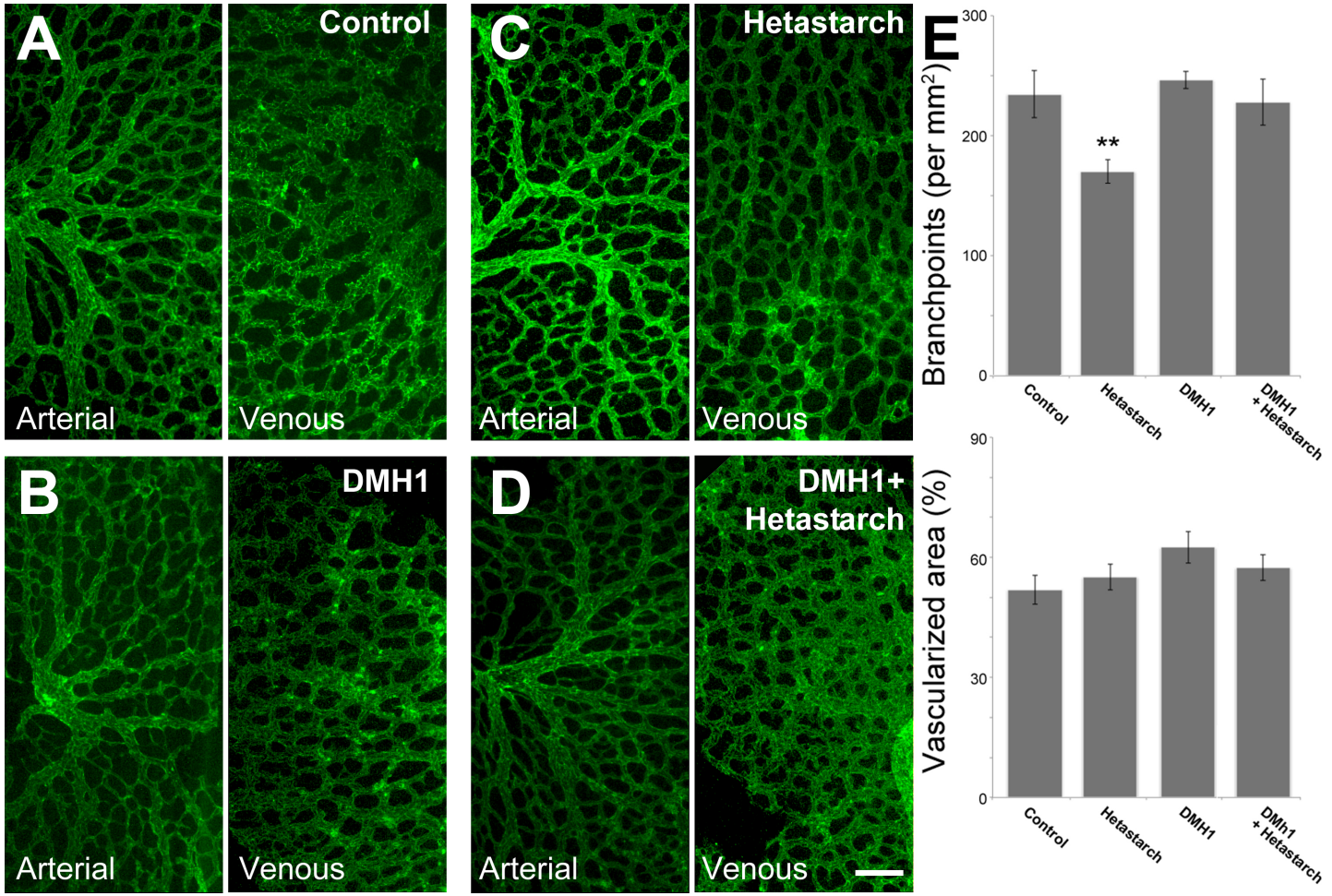
A
Control
Arterial
Venous
C
Hetastarch
Arterial
Venous
B
DMH1
Arterial
Venous
D
DMH1+
Hetastarch
Arterial
Venous
E
Branchpoints (per mm2)
300
200
100
0
**
Control
Hetastarch
DMH1
DMH1
+ Hetastarch
Vascularized area (%)
90
60
30
0
Control
Hetastarch
DMH1
DMH1
+ Hetastarch

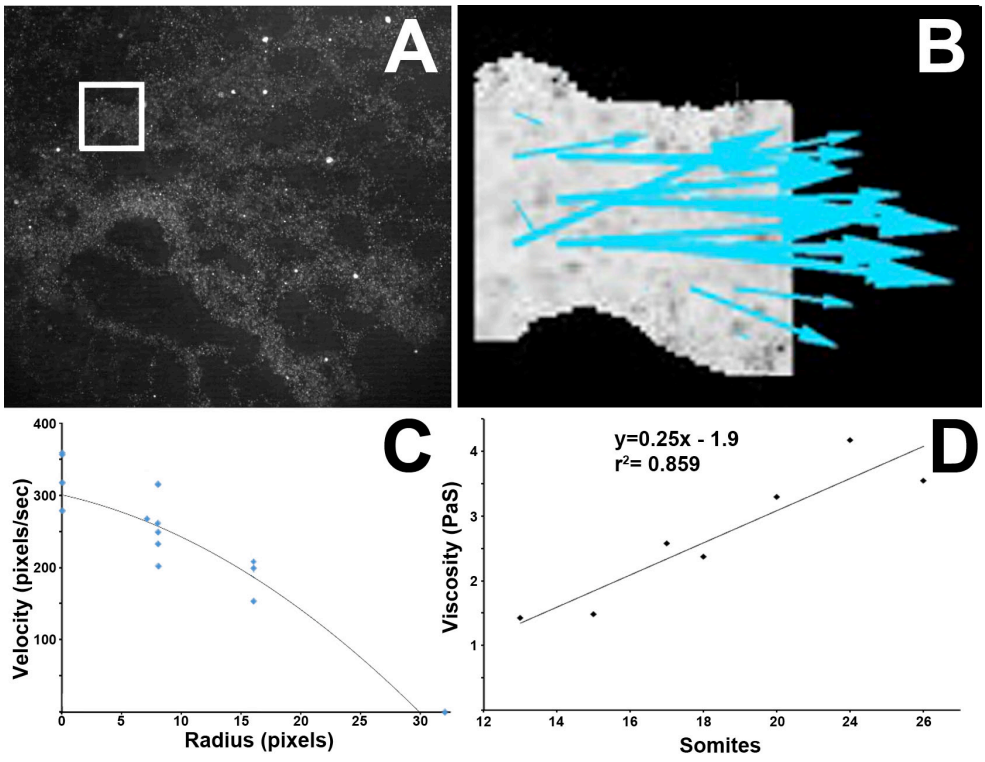

Supplemental Figure 1 – Measurement of Shear Rate and Hematocrit During Vascular Remodeling in Quail Embryos. Blood flow was seeded with fluorescent microspheres and the yolk sac capillary plexus was imaged with a 5x objective lens on a high-speed camera fluorescent microscope (A). Individual vessel segments were cropped from the images (box, A) and the motion of the microspheres were analyzed using micro Particle Image Velocimetry (B). The velocities within the blood vessel segment showed a parabolic velocity profile as expected (C), however the majority of measurements were near the center of the blood vessel and therefore the maximum velocity at the center of the vessel was used to calculate shear rates. Shear stress calculations also require knowledge of the viscosity of the flow. The viscosity is dependent on the hematocrit of the blood. We used a previously published technique [17] to measure the hematocrit of quail embryos at different stages of development and calculated the viscosity from the measured hematocrit (D).

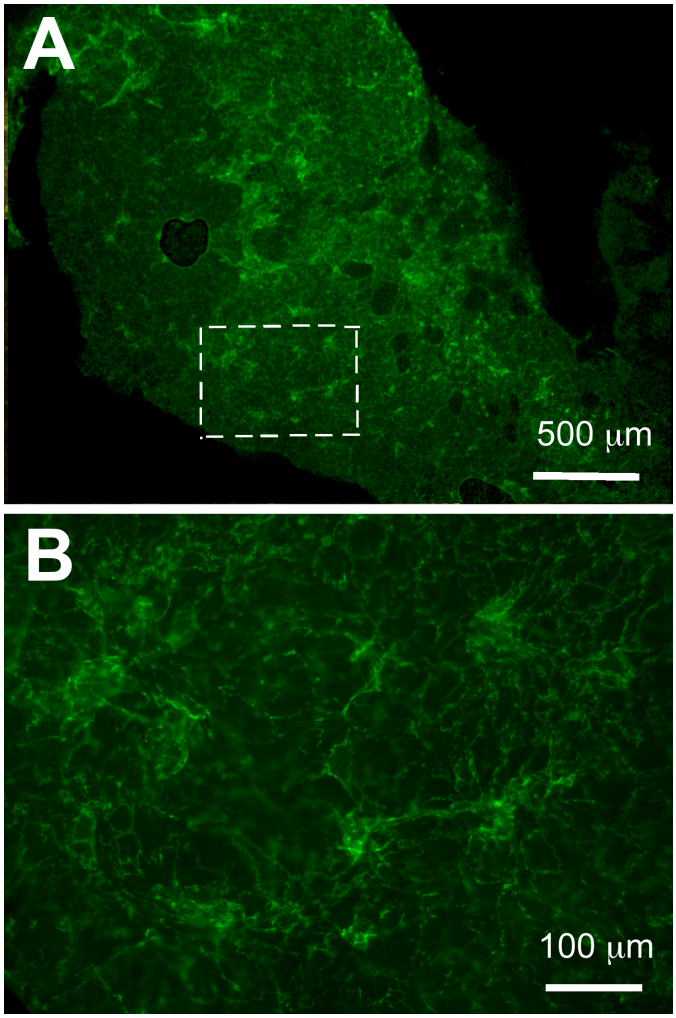

Supplemental Figure 2 – Regions of Intense CD31 Staining in DAPT Treated Embryos. In the most severe incidents, DAPT treatment caused large regions of the yolk sac to stain positive for CD31 (endothelial cells) with no avascular regions present. A higher magnification view of the dotted square (A) is shown in panel B.